Barriers shapes and minimum set of rotor parameters in the automated design of Synchronous Reluctance machines

Barriers shapes and minimum set of rotor parameters in the automated design of Synchronous Reluctance machines

G. Pellegrino, *Senior Member, IEEE*, F. Cupertino, *Senior Member, IEEE,* and C. Gerada, *Member, IEEE*

***Abstract*— The rotor design of Synchronous Reluctance machines is considered in this paper, based on a multi-objective, genetic optimization algorithm and finite element analysis. Three different types of barrier geometries are compared, all described by a limited set of input variables. The aim of the paper is to investigate the relationships between the obtainable performance and the different barrier types. The two questions underlying this analysis are: which is the geometry that can potentially give the machine with the highest torque to volume ratio? Which is the geometry with the best compromise between number of input parameters (i.e. computational time) and performance? The results of the analysis show that Synchronous Reluctance machines can be designed using artificial intelligence in a reasonable time, obtaining adequate performances and rotor geometries consistent with the literature.**

Index Terms — Synchronous reluctance machines, Rotor design, Design optimization, Pareto optimization

I. Introduction

SYNCHRONOUS Reluctance (SyR) motors are a viable alternative to inverter-driven Induction Motors (IM) because of their efficiency, lower rotor temperature and higher transient overload capability. SyR motors have been studied comprehensively since the 1990s [1,2] and their optimal design is also the basis for mastering the design of permanent magnet (PM) assisted SyR machines [3], a class of interior PM machines of particular interest nowadays [4].

The design of salient rotors with multiple flux barriers has been formalized through the years by many authors. A standard design is yet an open challenge, in particular for industry, where such rotor configurations are still very little known. The attempts to delegate the SyR machine design to artificial intelligence are discouraged by the long simulation time related to the execution of numerous finite element analysis (FEA) runs. Finite elements analysis is acknowledged to be necessary in the design of such machines, where magnetic saturation must be taken into account comprehensively and accurately. The number of FEA runs required to optimize one design is on the one hand related to the convergence of the optimization algorithm, meaning how many candidates must be evaluated before the algorithm converges to a solution. On the other hand, SyR machines have the singular property to require more than one FEA run for their performance to be evaluated. First of all, torque ripple is a mandatory goal to be included in the design and requires multiple rotor positions to be simulated. Second, the current phase angle giving the Maximum Torque per Ampere (MTPA) varies design by design and it is unknown a priori each time a new candidate machine is evaluated by the search algorithm. To give a counter example, Surface mounted PM machines can be evaluated via one static FEA simulation, like in [5], but this is not the case here.

As for the number of iterations required by the optimization algorithm to converge, the number of input variables defining the search space plays a key role. The number of geometric parameters required to describe a multi barrier SyR rotor varies in the literature and it is generally high, and also growing fast with the number of layers [9]. All considered, the joint application of FEA and optimization algorithms has been mostly experimented on simple, single-layer geometries [6-7]. Otherwise, it has led to admittedly long computational times [8-9].

In recent papers [10-11], FEA and multi-objective genetic algorithm (MOGA) optimization have been successfully associated to produce SyR and PM-assisted SyR designs in reasonable times. In [10] a set of key parameters capable of describing the rotor geometry with nearly no loss of performance is introduced, along with quick FEA evaluation of the machines. In [11], a procedure for designing SyR rotors with round barriers is formalized. Torque, torque ripple and the MTPA condition of the candidate machines are evaluated consistently via five static FEA simulations per each new candidate. Saliency maximization and power factor maximization are the byproducts of torque maximization. The computation required for a new design, starting from raw specifications such as volume constraints and heat dissipation capability is 17.5 hours on a 8-core Xeon Workstation. Tests on prototypes show that the torque is close to the benchmark of a state of the art design and the torque ripple is further improved [11].

This work develops the results obtained in [10-11] with circular barriers to flux barriers made of straight segments like the ones shown in Fig. 1. The effects of the barriers geometry on performance and of the number of input variables on the computation time are investigated. A refinement of the optimization procedure is also introduced and tested. The

This work was supported in part by project PON MALET – code PON01_01693.

G. Pellegrino is with the Politecnico di Torino, Torino, Italy (e-mail: gianmario.pellegrino@polito.it)

F. Cupertino is with the Politecnico di Bari, Bari, Italy (e-mail: cupertino@poliba.it)

C. Gerada is with the University of Nottingham, Nottingham, UK (e-mail: chris.gerada@nottingham.ac.uk)

angled barriers proposed here produce an output torque and a torque ripple that are comparable with the ones obtained in the past, within the same computational time. Yet, the new rotors are lighter and more robust structural wise. Last, standard rectangular PM pieces can be accommodated into saliencies of the kind of Fig. 1 very comfortably, while the circular barriers required custom cut or injection molded PMs.

II. 3U and I2U Rotor Geometries

In Fig. 1 the barriers are made of three straight segments, similar to the shape of a U. The three layer example, then called 3U rotor, is described by seven variables: two per layer, namely the barrier thicknesses (hc_{123}) and their angular positions at the airgap ($\Delta\alpha_{123}$), and one more, Δx, accounting for how deeply are the barriers positioned, radial wise. The bottom limit case $\Delta x = 0$ develops into one I-shaped barrier and it is hereinafter indicated as I2U (one I- plus two U-shaped barriers), represented in Fig. 2a. The upper limit $\Delta x = 1$ replicates the radial positions of three circular barriers having the same set of inputs (hc_{123} and $\Delta\alpha_{123}$), as reported in Fig 2b. It is impossible to move the barriers any further, radially, without introducing more degrees of freedom. Last, the rotors with circular barriers like the one indicated with black thin lines in Fig. 2 are named 3C rotors. They are the ones presented in [10-11] and are used here as a term of comparison.

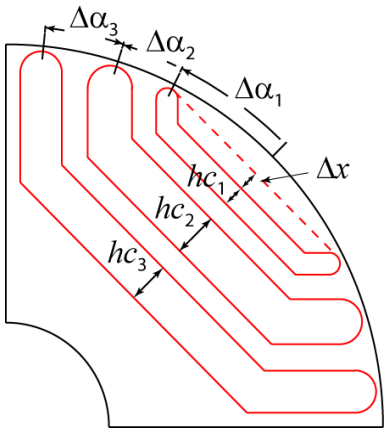

Fig. 1. Set of input parameters defining the 3U rotor geometry.

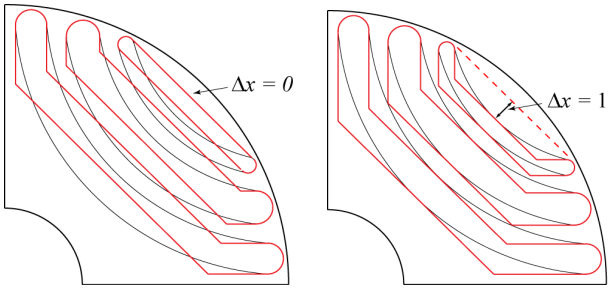

Fig. 2. Bottom (a) and top (b) extremes of the displacement parameter Δx. Rotor (a) is called I2U.

III. Torque and Torque Ripple Optimization

A. Problem parameterization

The number of parameters used to specify the rotor geometry has to be as low as possible so to simplify the optimization problem. To this aim some assumptions are made on the rotor geometry.

1. The end of all the flux barriers has been selected round shaped with a diameter equal to the thickness of the flux barrier.
2. All the considered geometries have rotor flux paths with constant thickness.
3. The structural ribs at airgap are of a fixed width that depends on punching limits and centrifugal stresses. A width of 0.5 mm was used during the optimization in this case and all the designed prototypes have been verified towards centrifugal stress at the maximum speed that is 8000 rpm in this case.

The I2U geometry is the one that better withstands centrifugal forces due to the reduced iron quantity in the peripheral areas of the laminations. Only 6 parameters specify the 3C and I2U geometries and an additional parameter is required for the generic 3U rotors, other than I2U, as explained in the previous section. A per unit representation of the set of parameters together with a correct choice of the search bounds, allows MOGA to place the layers in any position but avoiding unfeasible rotors (a minimum distance between the layers has to be guaranteed for manufacturing).

B. Figures of merit and goals of the optimization

The performance indexes to be optimized by the MOGA are the torque and torque ripple, evaluated at a single current amplitude and phase angle so to reduce computation. The current amplitude level selected in the examples is twice the machine rated current, as a trade-off between continuous torque and maximum overload conditions. Moreover, preliminary investigations revealed that machine with a good torque/torque ripple compromise in overload conditions are likely to perform well also with lower current levels, and not vice-versa, because machines optimized at lower currents have a tendency to perform badly at overload.

Dealing with the current phase angle, named γ and referred to the *d-q* synchronous frame, the evaluation of the motor torque capability requires the knowledge of the MTPA condition. This is represented by the angle γ_{MTPA}, at the selected current level. Instead of questing for the best γ angle for each candidate machine with simulations at different phase values, we include the phase angle among the parameters to be optimized by the MOGA: each machine is then evaluated at a single current angle, as said, and this is selected randomly by MOGA. After the optimization algorithm has optimized torque ripple and average torque, it happens for all the machines of the final Pareto front that

1. the γ_{MTPA} angle is correctly estimated by MOGA,
2. the torque ripple of all output machines is minimized with particular evidence along the MTPA trajectory, at all current amplitudes.

Torque ripple is evaluated as the standard deviation of torque at n equally spaced rotor positions over one stator slot

pitch (τ_{st}). The stator slot pitch is representative of the most significant torque ripple harmonic component, with windings of the distributed type. Dealing with the torque ripple waveform, the number of simulations required to avoid the aliasing of significant torque harmonics is discussed in [10]. The introduction of a random offset position allows the correct evaluation of first and third torque ripple harmonics with 5 positions simulated over the stator slot pitch.

C. Genetic optimization procedure

The proposed MOGA-based design procedure consists of a first stage called global search (GS) and a successive local search refinement stage (LS). Both stages are executed utilizing the NSGAII algorithm included in Matlab Optimization Toolbox. During the GS, the bounds of the search space are kept quite large, meaning that all the feasible rotors are considered as possible solutions. Table I reports the numerical values of the bounds used for the GS. The angle $\Delta\alpha_1$ is expressed in degrees, while the other two angles $\Delta\alpha_2$ and $\Delta\alpha_3$ are expressed in p.u. This means that is the two p.u. angles are equal, the flux barriers tips are uniformly distributed at airgap, between $\Delta\alpha_1$ and 90 degrees. If $\Delta\alpha_2$ is smaller than $\Delta\alpha_3$ the tip of the middle barrier will be closer to the external one and vice-versa. After the positioning of barrier tips, their thickness is imposed using the h_{c123} expressed in p.u.. If it happens that the barriers overlap and there is no space left for the steel flux tube in between, their thickness is decreased until a minimum clearance of 1.0 mm is guaranteed. Finally, and only in the case of 3U geometry, parameter Δx is applied by moving all the barriers in the deeper part of the rotor without affecting barrier and flux path ticknesses.

The quality of the final solution found by GS is related to the amount of time dedicated to the search. Considering that the stochastic nature of genetic algorithms does not guarantee to find the optimal solution after each single run and aiming to reduce the overall computational burden, we propose to execute a number of short GS runs each of those require a limited computational time. In particular we used four GS runs with a population of 60 individuals iterated over 50 generations. Each GS run takes less than 2.5 hours on a 8-cores Xeon-based workstation or about 3.75 hours on a i7-based 4-cores laptop. At the end of the GS runs the most promising regions of the search space are evidenced even if the selected machines could be only roughly close to the optimal ones. The four Pareto fronts resulting from the GS runs are merged to form a set of preferred solutions. A single LS run with search bounds restricted so to consider only the solutions in the most promising search regions is then used for a refinement of the GS solutions. In particular, the search bounds used for LS are selected so to include the most promising GS solutions plus or minus a variation of 15% of each input parameter. The overall optimization procedure can be completed within 12.5 hours with the mentioned workstation. As an alternative procedure, to avoid the LS procedure, a number of long (computationally intensive) GS run would be needed. When the calculation of machine performances is performed by means of finite element simulations a single long run a with wide search space requires hundreds of thousands of simulations. The time needed to perform the machine design optimization would be several days and would make the use of the automatic procedure not-practical. The same design procedure has been applied to the design of rotors having 3C, 3U and I2U geometries.

IV. MOGA Results

The results of the GS+LS procedure are reported in Fig. 3 for three example geometries. With reference to the three subfigures:

a) Is the benchmark MOGA rotor with circular barriers (3C).
b) Is the 3U geometry with all the seven variables optimized, including the radial depth Δx. This one is indicated as 3U.
c) Is the 3U geometry optimized with Δx set to zero, producing a I2U machine.

It is evident from Fig. 3 that the angular positions and thicknesses of the barriers of 3U are very similar to the ones of 3C. Moreover, the barriers of 3U are not intrusive at all, radial-wise, meaning the factor Δx is close to zero and the 3U solution is close to a I2U rotor. This is consistent with the literature, because a large Δx would increase the permeance of all the air barriers (increased q-inductance) and also make the rotor flux tubes longer and more subjecto to saturation (premature saturation of the d inductance). Last, the I2U rotor in Fig. 2c has $\Delta x = 0$, that is the MOGA handling only six degrees of freedom, as it was also for the 3C case. Also here the barriers positions and thicknesses of I2U are similar to the ones of the other two designs.

TABLE I
LIMITS OF THE SEARCH SPACE FOR THE GLOBAL SEARCH (GS)

Parameter	Min value	Max value	Units
hc_1	0.2	1	p.u.
hc_2	0.2	1	p.u.
hc_3	0.2	1	p.u.
$\Delta\alpha_1$	15	27	degrees
$\Delta\alpha_2$	0.33	0.67	p.u.
$\Delta\alpha_3$	0.33	0.67	p.u.
Δx	0	1	p.u.
γ	20	80	degrees

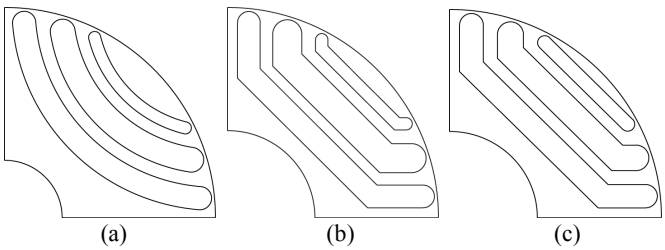

Fig. 3. MOGA designed rotors, with different shapes of the flux barriers. a) Round barriers (3C); b) 3U angled barriers, with the displacement factor Δx optimized; c) I2U angled barriers.

The torque waveforms represented in Figs. 4a to 6a show that the three designs have comparable torque and torque ripple levels at all current loads. The torque ripple is actually non negligible only at 300% load, but the reinforcement of the percent ripple with current loading and rate of saturation is again expected, according to the literature. Most of SyR machines are skewed, even when designed for low torque ripple.

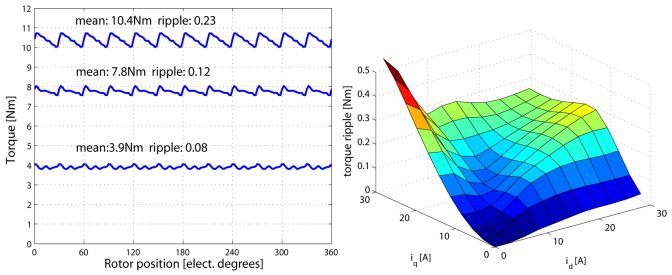

(a) (b)

Fig. 4. 3C optimal machine. a) Torque waveforms at 100%, 200% and 300% of rated current. b) Torque ripple surface

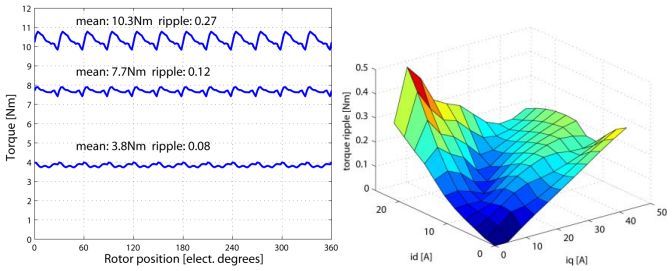

(a) (b)

Fig. 5. 3U optimal machine. a) Torque waveforms at 100%, 200% and 300% of rated current. b) Torque ripple surface

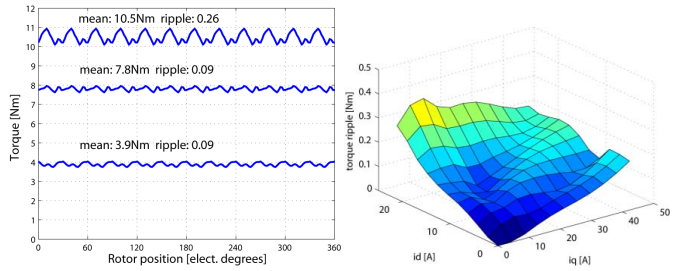

(a) (b)

Fig. 6. I2U optimal machine. a) Torque waveforms at 100%, 200% and 300% of rated current. b) Torque ripple surface

A. *Discussion of the number of inputs*

The ripple surfaces over the *dq* current plane show that the six-variables cases 3C and I2U give a lower ripple overall, with respect to the seven variables case 3U. This leads to the following conclusions:

1) the I2U geometry can have the same performance of the 3C one. The steel segment on top of the *q* axis, the one that tends to disappear when $\Delta x = 0$ and it is instead prominent with the circular barriers has little or no impact on performance.
2) A geometry of the I2U kind instead of the 3C can improve mechanical aspects such as the stress in the structural ribs and reduce the moment of inertia. Moreover, there is more room for the shaft.
3) The lower performance of the 3U with respect to the sub case I2U is accountable to the slower convergence of the MOGA when the additional degree of freedom Δx is used. We used the same problem size to keep the same computational time, and the results are a little worse, in this case.
4) The additional degree of freedom Δx is then giving little or no improvement in performance, but slows the convergence to the optimal solution. The best tradeoff between MOGA time and results for the 3U geometry is then the I2U machine.

B. *Improvement of the I2U local search stage*

Provided that the I2U geometry is the candidate for future developments of SyR and PM-assisted SyR designs, at least for two-pole pairs, the LS stage is further refined with the aim of improving the torque ripple also at current overload at the expense of a reasonable extra calculation. Two directions are explored, both starting from the same set of GS solutions used for the I2U design of Fig. 2.

The first attempt is called LS15, because the MOGA evaluates the torque ripple over 15 rotor positions instead of 5 in the LS stage. Five positions is the default used so far for both GS and LS. The optimization is run at 200% current load. The required extra time is 5 hours, because one LS run exploring 5 rotor positions takes 2.5 hours, and one with 15 positions takes 7.5 hours. The results, reported in Figs. 7 and 8, left hand side, say that the ripple is annihilated at 200% current, but not elsewhere: the optimization is too localized.

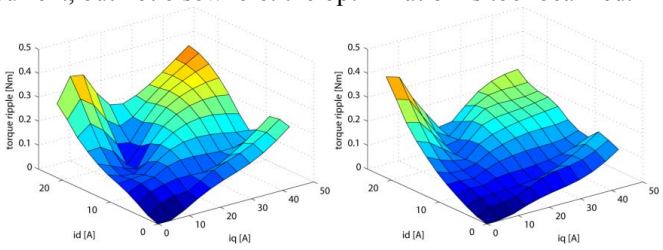

(a) (b)

Fig. 7. Examples of extra-time in the Local Search optimization: a) LS15, torque evaluated over 15 positions; b) LS5+5, torque evaluated over 5 positions and two current amplitudes.

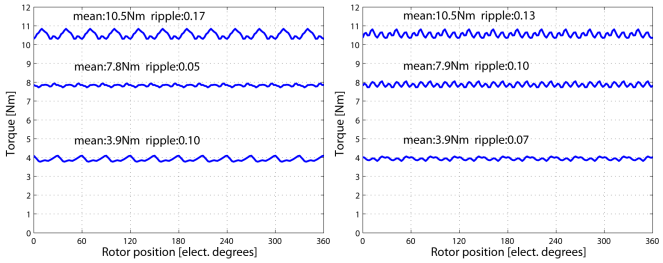

(a) (b)

Fig. 8. Torque waveforms of the two motors at Fig. 7, at 100%, 200% and 300% of rated current.

This is an interesting results because shows how sensitive is the final result to the conditions simulated during

optimization. The ideal optimization should evaluate the machine performance at different load condition, so to avoid the over-specialization of the final result as in Fig. 7a. Simulating the machine at more than one load level is unfeasible in terms of computational effort. A way to obtain better results in a reasonable time is to use two current levels only during the local search refinement. The torque waveform of each candidate is again evaluated over 5 positions, but at two different loads: 100% and 300%. This case is called LS5+5, and takes 2.5 hours extra time (5 hours for the LS5+5 run). Figs. 7b and 8b confirm that the torque ripple is better than it was in Fig. 6, also at 300% overload, and that the average torque is unchanged. The torque ripple surface is very regular, and it is minimized exactly along the MTPA trajectory in the i_d, i_q plane, that is one of the features of the proposed method.

V. EXPERIMENTAL RESULTS

Two SyR rotor prototypes have been purposely built for validating the proposed design procedure. Figure 9 reports the pictures of the respective laminations. The one in subfigure (a) is the 3C rotor presented in [11], while the one in subfigure (b) is the I2U rotor obtained with the GS followed by the LS5+5 refinement. It must be remarked that all the corners of the flux barriers of the I2U prototype are filleted with a radius of 1mm, that make then the lamination different from the ones calculated by the MOGA. When re-evaluating the machine performance in post-processing, the fillets have been included in the FEA model used for comparison with the experimental results.

TABLE I
MAIN PARAMETERS OF PROTOTYPES

Quantity	Value
Stator slots	24
Pole pairs	2
Rotor diameter	58.58 mm
Stator diameter	101 mm
Stack length	65 mm
Airgap	0.5 mm
Rated current (pk)	13.6 A
Rated voltage (dc-link)	300 V
Maximum speed	8000 rpm

(a) (b)

Fig. 9. Rotor laminations of prototype 3C (a) and prototype I2U (b).

In other words, the FEA results from now on refer to the actual prototype drawing, and gives marginal differences in terms of torque and ripple with respect to the ones calculated by the MOGA. Actually, the fillets tend to improve the performance rather than the opposite, and this stands for the robustness of the proposed method towards little modifications due to tolerances and non idealities. This is not the case with the 3C prototype, that does not need any modifications of the drawing. The most relevant parameters of the prototyped machines are reported in table I.

A. Experimental setup

The maps of the torque ripple versus the i_d and i_q current components have been measured for both prototypes using a dedicated test bench. A DC motor having very low torque ripple is coupled to the motor under test using a gearbox with reduction ratio equal to 50. The shaft torque is measured using a high precision torque meter. The geared DC motor is speed controlled and the torque is then measured at a constant speed of 10 rpm. The motor under test is vector current controlled, using a dSPACE 1104 board. A Matlab script has been realized to set the current references automatically and measure the torque during one motor revolution. The torque-meter rating has imposed not to exceed the 30 A per 20 A current area. The test bench is shown in Fig. 10.

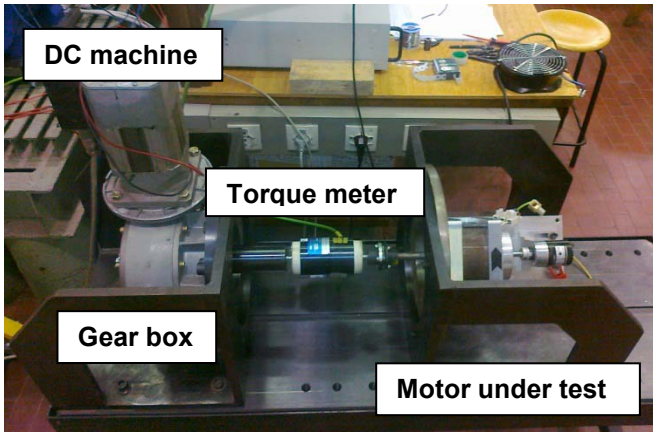

Fig. 10. Test bench used to measure the torque ripple maps of the motor prototypes.

B. Results discussion

In order to compare FEA and experimental results, the torque contours in the i_d-i_q plane are reported in Figs. 11 and 15 for the two machines, 3C and I2U respectively. For both machines there is a very good agreement between simulations and experiment for low torque values up to rated torque, is 4 Nm, corresponding to the rated current in Table I. The discrepancy between FEA and experiments grows as the load level is increased, as evident from the torque maps The difference between FEA and experiments is below 6.5% at 8 Nm and can be caused by many factors: steel model, an actual airgap that is higher than the FEA evaluated one, etc… At the time of writing, this point is still under investigation.

Figs. 12 and 16 report the average torque as a function of the current phase angle for two current levels equal to 16.8 A and 32.5A. These results further confirm the good agreement of simulations and experiment, with a little difference in terms of average torque and the MTPA phase angles practically the

same between the simulated and the prototyped machines.

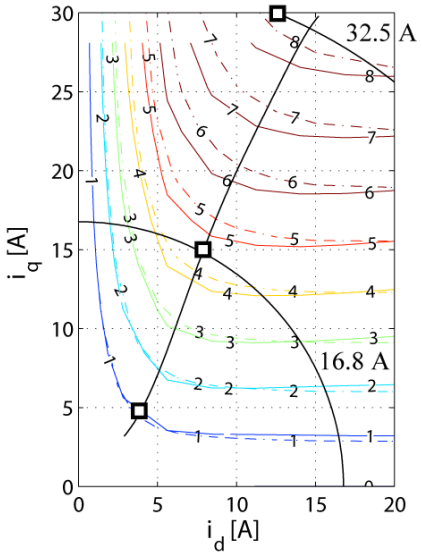

Fig. 11. Prototype 3C: torque contours evaluated with FEA (continuous line) and with measures (dash – dot lines). The MTPA line is in evidence. The three squares indicate the working points reported in Fig. 14.

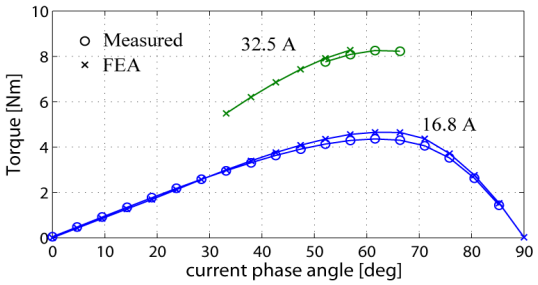

Fig. 12. Prototype 3C: average torque as a function of the current phase angle, as two different values of current amplitude.

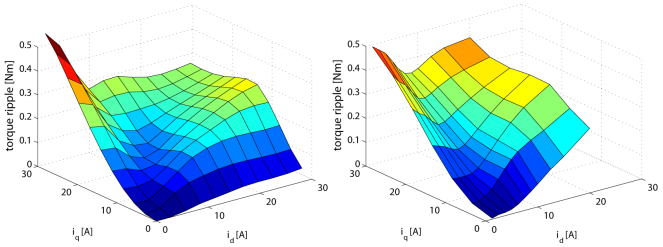

(a) (b)

Fig. 13. Prototype 3C: torque ripple surface over the id, iq plane, according to FEA (a) and measurements (b).

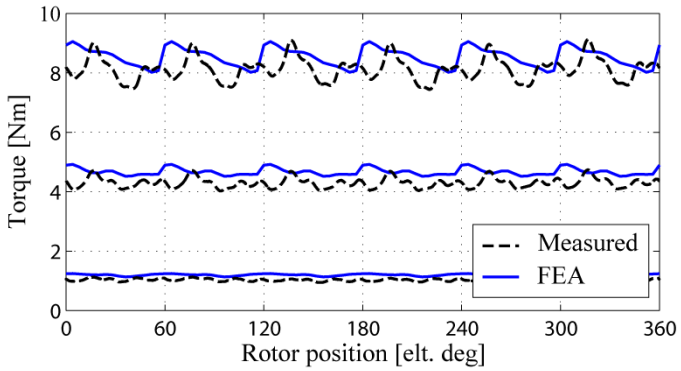

Fig. 14. Prototype 3C: torque waveforms on the MTPA.

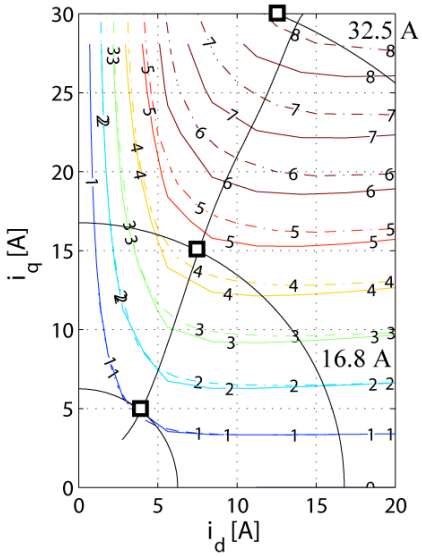

Fig. 15. Prototype I2U: torque contours evaluated with FEA (continuous line) and with measures (dash – dot lines). The MTPA line is in evidence. The three squares indicate the working points reported in Fig. 18.

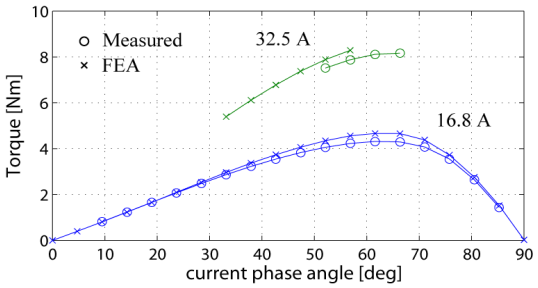

Fig. 16. Prototype I2U: average torque as a function of the current phase angle, as two different values of current amplitude.

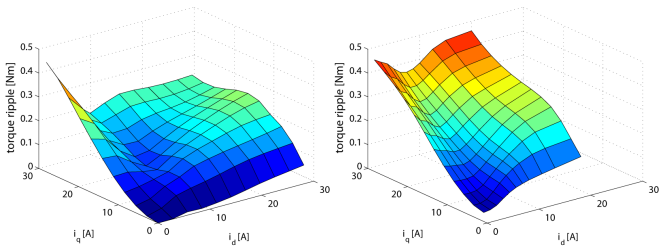

(a) (b)

Fig. 17. Prototype I2U: torque ripple surface over the id, iq plane, according to FEA (a) and measurements (b).

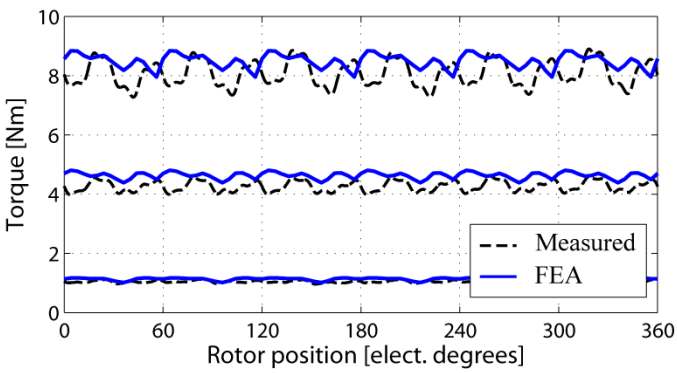

Fig. 18. Prototype I2U: torque waveforms on the MTPA.

The MTPA trajectory in the i_d-i_q plane is evidenced with black lines in figures 11 and 15. Figures 13 and 17 compare the torque ripple surfaces in the i_d-i_q plane according to FEA and measurements. As evidenced in the case of average torque, also for the torque ripple there is a good agreement for currents up to 15 A, then the measured ripple tends to be higher than the value predicted by simulations. It is mostly the i_d that makes the difference, both in the torque maps and in the ripple maps. Nevertheless, both in FEA and in experiments there is a minimum ripple path in the i_d-i_q plane, and this is very close to the MTPA trajectory. This result is one of the most clear proofs of the effectiveness of the proposed design method.

Finally, Figs. 14 and 18 show the torque waveforms at three current levels, selected along the MTPA trajectory and evidenced with black squares in Figs. 11 and 15. Considering that the prototyped machines are not skewed, the torque ripple is limited also at overload and also in experiments.

The overall good agreement of FEA and experimental results together with the absolute good performances of the prototypes in terms of torque density and torque ripple confirm the feasibility of the proposed MOGA assisted design of synchronous reluctance machines.

VI. CONCLUSION

This paper presents a procedure for the automatic design of multi-layer synchronous reluctance rotors based on FEA and assisted by MOGA. In the paper, two geometries described by six degrees of freedom give better results than one with seven degrees of freedom. This confirms that trying to complicate the description of the rotor geometry gives a little potential in terms of torque, at the expense of the certainty of a worse convergence of the genetic algorithm, The study demonstrates that geometries with two parameters per each flux barrier, the barrier angular position at airgap and its thickness, are a good tradeoff between performance and time.

The consistency of the torque-ripple optimization has been tested at very different load levels and on different rotor geometries. The uniformity of the torque ripple optimization over the current plane has been improved, and the extra simulation time quantified.

The selected rotor geometries (3C and I2U) can be described with the same set of six parameters. The I2U geometry is an original contribution of the paper and allows to reduce centrifugal stresses on rotor ribs with respect to the previously experienced 3C geometry. Moreover the I2U rotor is better suited for sintered magnet insertion in flux barriers to realize internal permanent magnet machines with wide constant power speed range and improved power factor that are the subject of the ongoing research.

REFERENCES

[1] T. A. Lipo, T. J. E. Miller, A. Vagati, I. Boldea, L. Malesani, and T. Fukao, “Synchronous reluctance drives,” in Conf. Rec. IEEE IAS Annu. Meeting, Denver, CO, Oct. 1994.

[2] RR Moghaddam, “Rotor for a Synchronous Reluctance Machine”, US Patent App. 13/230,543, 2011

[3] W. Soong and T. J. E. Miller, “Field weakening performance of brushless synchronous AC motor drives,” Proc. IEE—Elect. Power Appl., vol. 141, no. 6, pp. 331–340, Nov. 1994.

[4] Ooi, S.; Morimoto, S.; Sanada, M.; Inoue, Y.; , “Performance evaluation of a high power density PMASynRM with ferrite magnets,” Energy Conversion Congress and Exposition (ECCE), 2011 IEEE , vol., no., pp.4195-4200, 17-22 Sept. 2011

[5] Bianchi, N.; Bolognani, S., “Design optimisation of electric motors by genetic algorithms,” Electric Power Applications, IEE Proceedings - , vol.145, no.5, pp.475-483, Sep 1998.

[6] Dong-Joon Sim; Dong-Hyeok Cho; Jang-Sung Chun; Hyun-Kyo Jung; Tae-Kyoung Chung; , “Efficiency optimization of interior permanent magnet synchronous motor using genetic algorithms,” Magnetics, IEEE Transactions on , vol.33, no.2, pp.1880-1883, Mar 1997

[7] Sizov, G.Y.; Ionel, D.M.; Demerdash, N.A.O.; , “Multi-objective optimization of PM AC machines using computationally efficient - FEA and differential evolution,” Electric Machines & Drives Conference (IEMDC), 2011 IEEE International , vol., no., pp.1528-1533, 15-18 May 2011

[8] Kamper, M.J.; Van der Merwe, F.S.; Williamson, S.; , “Direct finite element design optimisation of the cageless reluctance synchronous machine,” Energy Conversion, IEEE Transactions on , vol.11, no.3, pp.547-555, Sep 1996

[9] Wen Ouyang; Zarko, D.; Lipo, T.A., “Permanent Magnet Machine Design Practice and Optimization,” Industry Applications Conference, 2006. 41st IAS Annual Meeting. Conference Record of the 2006 IEEE , vol.4, no., pp.1905-1911, 8-12 Oct. 2006

[10] Pellegrino, G.; Cupertino, F., “FEA-based multi-objective optimization of IPM motor design including rotor losses,” Energy Conversion Congress and Exposition (ECCE), 2010 IEEE , vol., no., pp.3659-3666, 12-16 Sept. 2010

[11] Cupertino, F.; Pellegrino, G.; Armando, E.; Gerada, C., “A SyR and IPM machine design methodology assisted by optimization algorithms” Energy Conversion Congress and Exposition (ECCE), 2012 IEEE , vol., no., 15-20 Sept. 2012.